

Nonlinear longitudinal current of band-geometric origin in wires of finite thickness

Robin Durand,¹ Louis-Thomas Gendron,¹ Théo Nathaniel Dionne,¹ and Ion Garate¹

¹*Département de physique, Institut quantique and Regroupement Québécois sur les Matériaux de Pointe, Université de Sherbrooke, Sherbrooke, Québec J1K 2R1, Canada*

(Dated: November 28, 2024)

The miniaturization of integrated circuits is facing an obstruction due to the escalating electrical resistivity of conventional copper interconnects. The underlying reason for this problem was unveiled by Fuchs and Sondheimer, who showed that thinner wires are more resistive because current-carrying electrons encounter the rough surfaces of the wire more frequently therein. Here, we present a generalization of the Fuchs-Sondheimer theory to Dirac and Weyl materials, which are candidates for next-generation interconnects. We predict a nonlinear longitudinal electric current originating from the combined action of the Berry curvature and non-specular surface-scattering.

Introduction.— A strong research effort is currently underway to find new interconnect materials that will replace copper in integrated circuits [1, 2]. Topological materials, endowed with their robust and highly conducting surface states, have the potential [3–7] to overturn the unfavorable resistivity scaling predicted by Fuchs [8] and Sondheimer [9] for conventional wires.

In this work, we generalize the Fuchs-Sondheimer (FS) theory to materials with nonzero electronic Berry curvature. For a homogeneous wire with time-reversal symmetry, we predict an electric current of band-geometric origin along the wire axis, which is quadratic in the applied electric field. While nonlinear Hall effects produced by the Berry curvature [10, 11] have been observed [12, 13], the nonlinear longitudinal current found below is fundamentally different. It emerges from the combined action of the Berry curvature and the non-specular scattering at the wire boundaries. Earlier studies [14–17] of nonlinear currents associated to the quantum metric tensor have ignored wire boundaries, therefore overlooking the effect we predict.

Methodology.— We consider conducting materials with low-energy electronic valleys. The electronic energy dispersion in the vicinity of valley χ is denoted as $\varepsilon_{\mathbf{p}}^{\chi}$, where \mathbf{p} is the momentum measured from the valley center. The system is finite in the z direction, $z \in [-a/2, a/2]$, but infinite in the remaining directions. We assume that there is only one band (per valley) that intersects the Fermi energy, therefore (i) neglecting size quantization effects (a must be much larger than the Fermi wavelength), and (ii) omitting the potential presence of topological surface states (we focus on the transport properties of bulk electrons).

The semiclassical transport under a uniform and constant electric field, $\mathbf{E} = E_x \hat{\mathbf{x}}$, is described by the Boltzmann equation

$$\dot{\mathbf{r}}_{\mathbf{p}}^{\chi} \cdot \nabla_{\mathbf{r}} f_{\mathbf{p}}^{\chi}(\mathbf{r}) + \dot{\mathbf{p}} \cdot \nabla_{\mathbf{p}} f_{\mathbf{p}}^{\chi}(\mathbf{r}) = \mathcal{I}_{\mathbf{p}}^{\chi}, \quad (1)$$

where $f_{\mathbf{p}}^{\chi}(\mathbf{r})$ is the electronic occupation,

$$\begin{aligned} \dot{\mathbf{r}}_{\mathbf{p}}^{\chi} &= \mathbf{v}_{\mathbf{p}}^{\chi} + \dot{\mathbf{p}} \times \boldsymbol{\Omega}_{\mathbf{p}}^{\chi} / \hbar \\ \dot{\mathbf{p}} &= -e\mathbf{E} \end{aligned} \quad (2)$$

are the electronic group velocity and force, $\mathbf{v}_{\mathbf{p}}^{\chi} = \nabla_{\mathbf{p}} \varepsilon_{\mathbf{p}}^{\chi}$, $\boldsymbol{\Omega}_{\mathbf{p}}^{\chi}$ is the Berry curvature in valley χ and

$$\mathcal{I}_{\mathbf{p}}^{\chi} = -\frac{1}{\rho(\varepsilon_{\mathbf{p}}^{\chi})\tau} \sum_{\mathbf{p}'} \delta(\varepsilon_{\mathbf{p}} - \varepsilon_{\mathbf{p}'}) (f_{\mathbf{p}}^{\chi} - f_{\mathbf{p}'}^{\chi}) \quad (3)$$

is the collision integral describing elastic scattering with bulk impurities in the lowest Born approximation. Here, τ is the mean scattering time and $\rho(\varepsilon)$ is the density of states at energy ε . Treating the valleys independently is justified if the intravalley scattering time is much shorter than the intervalley scattering time, which we assume to be the case for the sake of simplicity. Likewise, we neglect skew-scattering and side-jump processes.

We solve Eq. (1) perturbatively in powers of E_x up to second order, $f_{\mathbf{p}}^{\chi} \simeq f_{0,\mathbf{p}}^{\chi} + f_{1,\mathbf{p}}^{\chi} + f_{2,\mathbf{p}}^{\chi}$, where $f_{n,\mathbf{p}}^{\chi} \propto E_x^n$. For $n \geq 1$, we apply the boundary condition of Fuchs and Sondheimer [8, 9]: $f_{n,\mathbf{p}}^{\chi}(x, y, -a/2) = 0$ if $v_{\mathbf{p},z}^{\chi} > 0$, and $f_{n,\mathbf{p}}^{\chi}(x, y, a/2) = 0$ if $v_{\mathbf{p},z}^{\chi} < 0$. Physically, the electron distribution on each valley is in equilibrium immediately after a collision with the wire boundary. In the boundary conditions, $v_{\mathbf{p},z}^{\chi}$ appears instead of $\dot{z}_{\mathbf{p}}^{\chi}$; this is a consequence of solving Eq. (1) perturbatively in E_x .

Our quantity of interest is the longitudinal electric current density

$$j_x(\mathbf{r}) = \sum_{\chi} j_x^{\chi}(\mathbf{r}) = -e \sum_{\chi} \int \frac{d^d p}{(2\pi\hbar)^d} \dot{x}_{\mathbf{p}}^{\chi} f_{\mathbf{p}}^{\chi}(\mathbf{r}), \quad (4)$$

where d is the dimensionality of the system and j_x^{χ} is the valley-resolved current density along x . Note that Eq. (4) does not include the contribution from the orbital magnetic moment of electrons [18]. More precisely, we omit the contribution to the current coming from the part of $f_{\mathbf{p}}^{\chi}$ that is isotropic in \mathbf{p} [19]. Yet, this omission does not change the main prediction of our paper.

Broken translational symmetry along z implies $f_{\mathbf{p}}^{\chi}(\mathbf{r}) = f_{\mathbf{p}}^{\chi}(z)$ and thus $j_x(\mathbf{r}) = j_x(z)$. We write

$$j_x(z) \simeq \sum_{\chi} [j_{1,x}^{\chi}(z) + j_{2,x}^{\chi}(z)] = j_{1,x}(z) + j_{2,x}(z), \quad (5)$$

where $j_{n,x}(z) \propto E_x^n$. The effective linear ($\bar{\sigma}_1$) and nonlinear ($\bar{\sigma}_2$) conductivities are obtained by averaging

the current density over the wire thickness,

$$\bar{j}_x = \frac{1}{a} \int_{-a/2}^{a/2} dz j_x(z) \simeq \bar{\sigma}_1 E_x + \bar{\sigma}_2 E_x^2. \quad (6)$$

Solution of Eq. (1).– At zeroth order in E_x , Eq. (1) yields $f_{\mathbf{p}}^x = f_{0,\mathbf{p}}^x$ and $\partial_z f_{0,\mathbf{p}}(z) = 0$. Using this, the Boltzmann equation at first order in E_x reads

$$v_{\mathbf{p},z}^x \frac{\partial f_{1,\mathbf{p}}^x}{\partial z} - e E_x \frac{\partial f_{0,\mathbf{p}}^x}{\partial p_x} = \mathcal{I}_{1,\mathbf{p}}^x, \quad (7)$$

where $\mathcal{I}_{1,\mathbf{p}}^x$ is given by Eq. (3) with $f \rightarrow f_1$. The second term on the left hand side acts as a source term that forces $f_{1,\mathbf{p}}^x \neq 0$. Assuming that $\varepsilon_{\mathbf{p}}^x$ is invariant under $p_x \rightarrow -p_x$, the source term is odd in p_x . Hence, we can decompose f_1 in a part that is even in p_x and a part that is odd, only the latter being nonzero according to Eq. (7). Further imposing the FS boundary conditions, we reach

$$f_{1,\mathbf{p}}^x = \begin{cases} h_{1,\mathbf{p}}^x \left(1 - e^{-(z+a/2)/v_{\mathbf{p},z}^x \tau} \right), & v_{\mathbf{p},z}^x > 0 \\ h_{1,\mathbf{p}}^x \left(1 - e^{-(z-a/2)/v_{\mathbf{p},z}^x \tau} \right), & v_{\mathbf{p},z}^x < 0 \end{cases}, \quad (8)$$

where

$$h_{1,\mathbf{p}}^x \equiv e E_x \tau \frac{\partial f_{0,\mathbf{p}}^x}{\partial p_x}. \quad (9)$$

The electronic occupation becomes z -dependent at linear order in E_x . This position-dependence is significant only in the proximity to $z = a/2$ (for $v_{\mathbf{p},z}^x < 0$) and $z = -a/2$ (for $v_{\mathbf{p},z}^x > 0$). Far enough from the wire surfaces, Eq. (8) converges to the standard expression for infinite systems, $h_{1,\mathbf{p}}^x$, independent of z . These results are identical to the ones obtained by Fuchs and Sondheimer [8, 9], i.e. unaffected by the Berry curvature of electrons.

New results arise at second order in E_x , where the Boltzmann equation reads [19]

$$v_{\mathbf{p},z}^x \frac{\partial f_{2,\mathbf{p}}^x}{\partial z} + \frac{e E_x \Omega_{\mathbf{p},y}^x}{\hbar} \frac{\partial f_{1,\mathbf{p}}^x}{\partial z} - e E_x \frac{\partial f_{1,\mathbf{p}}^x}{\partial p_x} = \mathcal{I}_{2,\mathbf{p}}^x. \quad (10)$$

Here, the y -component of the Berry curvature appears in a source term for f_2 . Now, the two source terms (involving $\partial_z f_1^x$ and $\partial_{p_x} f_1^x$, respectively) do not in general have the same parity under $p_x \rightarrow -p_x$. Therefore, if we decompose f_2 in a part that is even in p_x and a part that is odd (once again under the assumption of $\varepsilon_{\mathbf{p}}^x$ being an even function of p_x), both parts are nonzero according to Eq. (7). The collision term for the even part cannot be solved analytically without invoking approximations that violate conservation laws. Fortunately, for the electric current in Eq. (4), only the part of f_2 that is odd in p_x matters [20]. This part can be analytically obtained [19] without resorting to approximations:

$$f_{2,\mathbf{p}}^x \ni \begin{cases} h_{2,\mathbf{p}}^x(z+a/2) e^{-(z+a/2)/v_{\mathbf{p},z}^x \tau}, & v_{\mathbf{p},z}^x > 0 \\ h_{2,\mathbf{p}}^x(z-a/2) e^{-(z-a/2)/v_{\mathbf{p},z}^x \tau}, & v_{\mathbf{p},z}^x < 0, \end{cases} \quad (11)$$

where

$$h_{2,\mathbf{p}}^x \equiv \frac{e^2 E_x^2 \Omega_{\mathbf{p},y}^x}{\hbar (v_{\mathbf{p},z}^x)^2} \frac{\partial f_{0,\mathbf{p}}^x}{\partial p_x}. \quad (12)$$

Interestingly, Eq. (11) is proportional to the y -component of the Berry curvature and emerges because $f_{1,\mathbf{p}}^x$ is z -dependent. Unlike $f_{1,\mathbf{p}}^x$, $f_{2,\mathbf{p}}^x$ is negligible far enough from the wire edges. In our theory, the absence of an $O(E_x^2)$ current far from the edges is a consequence of the assumed invariance of $\varepsilon_{\mathbf{p}}^x$ under $p_x \rightarrow -p_x$. When this assumption is relaxed, we find that there can be an additional $O(E_x^2)$ current density independent of Berry curvature for all z , provided that the crystal lacks time-reversal symmetry [21]. More so, should we incorporate skew-scattering processes in our theory, an $O(E_x^2)$ current density could likewise emerge for all z even if $\varepsilon_{\mathbf{p}}^x$ were invariant under $p_x \rightarrow -p_x$, and even in non-magnetic crystals [22].

Equation (11) foreshadows a nonlinear, surface-localized longitudinal current that originates from the joint presence of nontrivial band geometry and diffusive scattering at the wire's surfaces. The precise form of that current is system-dependent. To make further progress, we next focus on Dirac and Weyl materials.

Two dimensional Dirac metal.– We consider a crystal with time-reversal symmetry \mathcal{T} and broken space inversion symmetry \mathcal{P} (e.g. a transition metal dichalcogenide monolayer) in the xz plane, with $x \in (-\infty, \infty)$ and $z \in [-a/2, a/2]$. We suppose that the Fermi energy ε_F intersects the conduction band, whose nondegenerate (due to broken \mathcal{P}) dispersion at valley χ ($\chi = \pm 1$) is approximated as

$$\varepsilon_{\mathbf{p}}^x = \sqrt{c^2 p^2 + m^2} + \alpha_z^x p_z. \quad (13)$$

Here, c is the Fermi velocity, $\mathbf{p} = (p_x, p_z)$ is the momentum measured from the band edge, m is the Dirac mass and α_z^x is the tilt velocity along the p_z direction. Since the two valleys are related by \mathcal{T} , we have $\alpha_z^x = \alpha_z \chi$ and a Berry curvature [23]

$$\Omega_{\mathbf{p}}^x = \chi \frac{m \hbar^2 c^2}{2 (c^2 p^2 + m^2)^{3/2}} \hat{\mathbf{y}}. \quad (14)$$

In addition, the model and the FS boundary conditions display a mirror symmetry \mathcal{M}_z about a plane perpendicular to z .

We compute $j_{2,x}^x(z)$, the contribution from valley χ to the nonlinear part of the longitudinal current, by combining Eqs. (14), (11) and (4). To zeroth order in α_z and at low temperature, we obtain [19]

$$j_{2,x}^x(z) \simeq \chi E_x^2 \frac{e^3}{8\pi^2 \hbar \varepsilon_F^2} \frac{m}{\varepsilon_F} \int_0^\pi \frac{d\theta}{\tan^2 \theta} \times \left[\left(z + \frac{a}{2} \right) e^{-\frac{z+a/2}{l \sin \theta}} - \left(-z + \frac{a}{2} \right) e^{-\frac{-z+a/2}{l \sin \theta}} \right], \quad (15)$$

where $l = c\tau(1 - m^2/\varepsilon_F^2)^{1/2}$ is an effective bulk mean free path due to impurity scattering.

Four properties of Eq. (15) are worth mentioning. First, $j_{2,x}^+(z) = j_{2,x}^-(-z)$, which is a consequence of the mirror symmetry \mathcal{M}_z . The same property is satisfied at first order in E_x , i.e. $j_{1,x}^+(z) = j_{1,x}^-(-z)$. As a consequence, $j_x(z) = \sum_\chi j_x^\chi(z) = j_x(-z)$ at all orders in E_x , which is expected because an electric field along x preserves \mathcal{M}_z .

Second, $j_{2,x}^\chi(z) = -j_{2,x}^\chi(-z)$. This property can be understood mathematically from the fact that, in the absence of a tilt, the electronic dispersion (13) and the Berry curvature (14) of each valley are invariant under $(x, z; p_x, p_z) \rightarrow (-x, -z; -p_x, -p_z)$. Under this operation, $j_{2,x}^\chi(z) = \sigma_2 E_x^2 \rightarrow -j_{2,x}^\chi(-z) = \sigma_2' E_x^2$. From Neumann's principle [24], $\sigma_2 = \sigma_2'$ and therefore $j_{2,x}^\chi(z) = -j_{2,x}^\chi(-z)$. In contrast, $j_{1,x}^\chi(z) = \sigma_1 E_x \rightarrow -j_{1,x}^\chi(-z) = \sigma_1' (-E_x)$. Here, the symmetry condition $\sigma_1 = \sigma_1'$ leads to $j_{1,x}^\chi(z) = j_{1,x}^\chi(-z)$.

Third, $j_{2,x}^\chi(z)$ is localized near the edges of the wire. Such localization is directly associated to the second property, $j_{2,x}^\chi(z) = -j_{2,x}^\chi(-z)$. Indeed, far from the wire edges, the current density is expected to be spatially uniform and thus independent of z ; the relation $j_{2,x}^\chi(z) = -j_{2,x}^\chi(-z)$ then results in $j_{2,x}^\chi = -j_{2,x}^\chi = 0$ far from the edges. We emphasize that this localization of $j_{2,x}(z)$ near the edges takes place for bulk electrons, as our theory does not contain any surface-localized electronic bands. In addition, the localization length for $j_{2,x}^\chi(z)$ is of the order of the bulk mean free path, unlike what one would expect from surface-states. Such spatial distribution of $j_{2,x}^\chi(z)$ is contrary to that of $j_{1,x}^\chi(z)$: at first order in E_x , the current is distributed along the entire bulk of the wire (even far from the edges, as allowed by relation $j_{1,x}^\chi(z) = j_{1,x}^\chi(-z)$) and partially depleted at the surfaces of the wire due to diffusive scattering therein.

Fourth, $j_{2,x}^\chi(z)$ is equal in magnitude and opposite in sign for the two valleys. This is an immediate joint consequence of the first two properties. Therefore, $j_{2,x}(z) = \sum_\chi j_{2,x}^\chi(z) = 0$ for all z . This is again different to the situation at first order in E_x , where $j_{1,x}^\chi(z) = j_{1,x}^\chi(-z)$ and hence the two valleys contribute with equal magnitude and sign when $\alpha_z = 0$.

A physical picture for the second and third properties is sketched in Fig. 1. The Berry curvature leads to an anomalous velocity $\propto E_x \Omega_{\mathbf{p},y}^\chi$ along the z direction for electrons of momentum \mathbf{p} at valley χ . Consequently, the term $E_x \Omega_{\mathbf{p},y}^\chi \partial_z f_{1,\mathbf{p}}^\chi$ in Eq. (10) describes the leading order contribution of the anomalous velocity to the divergence of the electronic current density ($f_{1,\mathbf{p}}^\chi$ appears to leading order, because $\partial_z f_{0,\mathbf{p}}^\chi = 0$). Here, the word ‘‘contribution’’ is to be emphasized, as the total current density along z is zero (i.e., the integral of $E_x \Omega_{\mathbf{p},y}^\chi f_{1,\mathbf{p}}^\chi$ over \mathbf{p} vanishes). But, if we focus on electrons with momentum \mathbf{p} , their flow has a nonzero divergence in the vicinity of the wire edges (the flow is divergenceless far from the edges because $\partial_z f_1^\chi \simeq 0$ therein according to Eq. (8)). This implies an accumulation of electrons of a given \mathbf{p} near the wire edges.

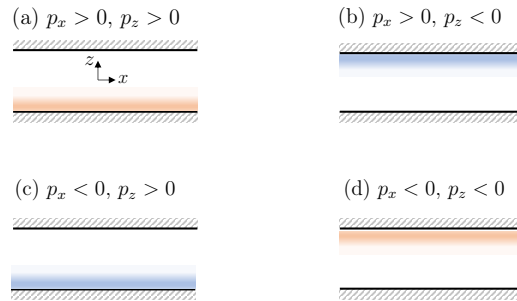


FIG. 1. Schematic contribution of the anomalous velocity to the electronic distribution function at a single valley of a 2D metal, as a function of the electronic momenta (p_x, p_z) . Orange: accumulation; blue: depletion; white: negligible contribution. Black solid lines denote the surfaces of the wire; grey dashed lines denote regions outside the wire. Regardless of p_z , there is an excess of right-moving electrons ($p_x > 0$) on one side of the wire and an excess of left-moving electrons ($p_x < 0$) on the opposite side of the wire.

To determine the nature of such accumulation, we notice that (i) for fixed p_z , $f_{1,\mathbf{p}}^\chi$ has opposite sign for $p_x > 0$ and $p_x < 0$ (this is expected as there is a net electric current along x at first order in E_x); (ii) for $p_z > 0$, $\partial_z f_{1,\mathbf{p}}^\chi$ is nonzero only near $z = -a/2$, while for $p_z < 0$, $\partial_z f_{1,\mathbf{p}}^\chi$ is nonzero only near $z = a/2$ (cf. Eq. (8)); (iii) for fixed p_x , $\partial_z f_{1,\mathbf{p}}^\chi$ switches sign under $p_z \rightarrow -p_z$ (this is again a consequence of the FS boundary conditions). It follows from (i), (ii) and (iii) that electrons with $p_x > 0$ and $p_x < 0$ accumulate on opposite edges of the wire (cf. Fig. 1). The accumulation takes place at order E_x^2 (one factor of E_x comes from the anomalous velocity, and the other from the spatial gradient of the electronic distribution function caused by diffusive boundary scattering). This is equivalent to a current distribution, which is quadratic in E_x , localized at the surfaces of the wires and antisymmetric with respect to the center of the wire. Hence, the second and third properties mentioned above are realized.

The presence of a tilt of the electronic structure along p_z changes some of the preceding properties qualitatively. Crucially, $\alpha_z \neq 0$ breaks the antisymmetry of $j_{2,x}^\chi(z)$ about the center of the wire (see Fig. 2). This is because $(x, z; p_x, p_z) \rightarrow (-x, -z; -p_x, -p_z)$ is no longer a symmetry when $\alpha_z \neq 0$. As a result, the two valleys no longer make mutually cancelling contributions to the nonlinear longitudinal current and $j_{2,x}(z)$ becomes nonzero. The relations $j_{n,x}^+(z) = j_{n,x}^-(-z)$ and $j_{n,x}(z) = j_{n,x}(-z)$ continue to hold for $n = 1, 2$ because the tilt along p_z preserves the mirror symmetry \mathcal{M}_z . Also, $j_{n,x}^\chi(z)$ and by extension $j_{2,x}(z)$ continue to be localized near the wire surfaces. In Ref. [19], we show an expression for $j_{2,x}(z)$ that is valid up to first order in α_z/c . This term scales as the product of α_z and the Berry curvature.

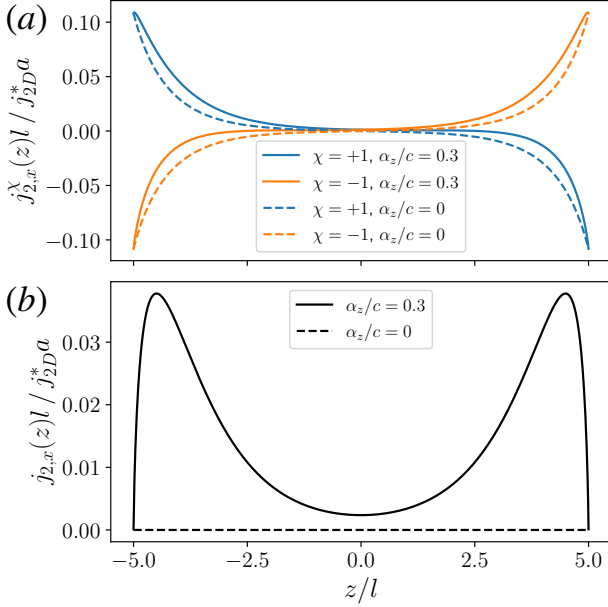


FIG. 2. Nonlinear longitudinal current density caused by the Berry curvature in a time-reversal-symmetric 2D Dirac metal with two electronic valleys ($\chi = \pm 1$). We take $a = 10l$ and $m = 0.5\varepsilon_F$. A tilt-independent normalization current $j_{2D}^* = j_{2D}c/\alpha_z$ is introduced, where j_{2D} is defined in the main text. (a) The valley-resolved current density $j_{2,x}^{\chi}(z)$ is localized near the wire edges, with a localization length of the order of l . In the absence of a tilt of the energy dispersion in the z direction ($\alpha_z = 0$), $j_{2,x}^{\chi}(z)$ is antisymmetric with respect to the center of the wire, and takes opposite values for the two valleys. A tilt $\alpha_z \neq 0$ skews the current density profile and prevents the cancellation between the two valleys. (b) The valley-summed nonlinear longitudinal current density $j_{2,x}(z)$ vanishes at every z when $\alpha_z = 0$. When $\alpha_z \neq 0$, $j_{2,x}(z)$ is nonzero and localized at the wire edges.

Combining the expression for $j_{2,x}(z)$ in [19] with Eq. (6), we obtain the nonlinear part of the current density averaged over the thickness of the wire at low temperature:

$$\overline{j_{2,x}} = \overline{\sigma_2} E_x^2 \simeq j_{2D} (1 - I), \quad (16)$$

where

$$I = \frac{3}{8} \int_0^\pi d\theta \frac{\cos^2 \theta}{\sin \theta} \left(\frac{a}{l} + 2 \sin \theta \right)^2 \exp\left(-\frac{a}{l \sin \theta}\right) \quad (17)$$

is a dimensionless integral and

$$j_{2D} \equiv E_x^2 \frac{16}{3} \frac{e^3}{\pi^2 \hbar^3} \frac{\varepsilon_F \Omega_y l^2}{c^2 a} \sqrt{1 - \frac{m^2}{\varepsilon_F^2} \frac{\alpha_z}{c}} \quad (18)$$

is proportional to the Berry curvature evaluated at the Fermi energy at valley $\chi = +1$, i.e. $\Omega_y = m\hbar^2 c^2 / 2\varepsilon_F^3$. This current reverses sign when time-reversal is applied to the system via $\alpha_z \rightarrow -\alpha_z$, $m \rightarrow -m$, $\tau \rightarrow -\tau$, $c \rightarrow -c$, with the other quantities remaining invariant. According

to conventional knowledge [25], there should not exist a current proportional to τ^2 in a crystal with \mathcal{T} , at least if skew-scattering is ignored [22]. Yet, such statement is no longer applicable when the electronic occupation varies in space, like in our case.

Analytical expressions of Eq. (16) are accessible in limiting regimes:

$$\overline{j_{2,x}} \simeq \begin{cases} j_{2D} & , a \gg l \\ 9a^2/(4l^2) \ln(l/a) j_{2D} & , a \ll l. \end{cases} \quad (19)$$

The fact that $\overline{\sigma_2} \propto 1/a$ when $a \gg l$ reflects the spatial localization of $j_{2,x}(z)$ near the wire edges, with a localization length that is independent of a . Thus, $\overline{\sigma_2} \rightarrow 0$ when $a \rightarrow \infty$. Likewise, $\overline{\sigma_2} \rightarrow 0$ in the $a \rightarrow 0$ limit, when the diffusive boundary scattering becomes pervasive. Given that $\overline{j_{2,x}}$ vanishes when $a \rightarrow 0$ and $a \rightarrow \infty$, it must have a maximum somewhere in between. The maximum of $\overline{\sigma_2}$, of value $\sim j_{2D}/E_x^2$, takes place at $a \sim l$. For $a \sim l$, $m \simeq 100\text{meV}$, $c \simeq 10^3\text{m/s}$ and $\alpha_z/c \simeq 0.3$, we find $\overline{\sigma_2}/\overline{\sigma_1} \simeq 10^{-3} \mu\text{m.volt}^{-1}$ [26]. Such ratio is similar to the one reported in the nonlinear Hall conductivity experiments (with the important difference that σ_2 is a longitudinal conductivity in our case).

Three dimensional Weyl metal.—Next, we consider a Weyl semimetal (WSM) [27] thin film in the xy plane, with $x, y \in (-\infty, \infty)$, and $z \in [-a/2, a/2]$. We start with two valleys of opposite chirality $\chi = \pm 1$, related by an improper crystal symmetry. We suppose that the Fermi energy ε_F intersects the conduction band. The electronic dispersion at valley χ is approximated as

$$\varepsilon_{\mathbf{p}}^{\chi} = cp + \alpha_y^{\chi} p_y + \alpha_z^{\chi} p_z, \quad (20)$$

where c is the Fermi velocity, $\mathbf{p} = (p_x, p_y, p_z)$ is the momentum measured from the Weyl point, α_y^{χ} and α_z^{χ} are tilt velocities at valley χ in the y and z directions, respectively. The Berry curvature for this model reads

$$\Omega_{\mathbf{p}}^{\chi} = \chi \hbar^2 \mathbf{p} / (2p^3). \quad (21)$$

Combining Eqs. (21), (11) and (4), we compute $j_{2,x}^{\chi}(z)$ [19]. Like in two dimensions, $j_{2,x}^{\chi}(z)$ is exponentially localized at the boundaries of the wire. In addition, if $\alpha_z^{\chi} = 0$, we find $j_{2,x}^{\chi}(z) = -j_{2,x}^{\chi}(-z)$, again like in the 2D Dirac metal. We notice, however, that $\alpha_y^{\chi} \neq 0$ is necessary for $j_{2,x}^{\chi}(z) \neq 0$, because $\Omega_{\mathbf{p},y}^{\chi}$ is an odd function of p_y in a Weyl semimetal.

Averaging the current density over the wire thickness, we get $\overline{j_{2,x}} = 0$ when either α_y^{χ} or α_z^{χ} are zero [19]. Thus, it is required that the Weyl cones be tilted in both directions transverse to the transport direction. This is analogous to what we found for a 2D Dirac metal. The two valleys make perfectly cancelling contributions to $\overline{j_{2,x}}$ if $\alpha_y^{\chi} \alpha_z^{\chi}$ is independent of χ ; such is the case when the two valleys are related to one another by a mirror plane perpendicular to the x -axis ($\alpha_z^+ = -\alpha_z^-$ and $\alpha_y^+ = -\alpha_y^-$). If the two valleys are instead related by a mirror plane perpendicular to the z axis, then

we have $\alpha_z^+ = -\alpha_z^-$ and $\alpha_y^+ = \alpha_y^-$. In such case, $j_{2,x}^+(z) = j_{2,x}^-(-z)$ and $\overline{j_{2,x}} \neq 0$.

In thick and thin films, we get

$$\overline{j_{2,x}} \simeq \begin{cases} j_{3D} & , a \gg l \\ 3a^2/(2l^2) \ln(l/a) j_{3D} & , a \ll l \end{cases} \quad (22)$$

to leading order in $|\alpha_y^x|/c$ and $|\alpha_z^x|/c$, with

$$j_{3D} \equiv E_x^2 \frac{e^3 l^2}{12 a h^2 c} \sum_{\chi} \chi \frac{\alpha_y^x \alpha_z^x}{c^2}. \quad (23)$$

Thus, $\overline{j_{2,x}}$ vanishes when $a \rightarrow \infty$ and $a \rightarrow 0$, its maximum of value $j_{3D}/2$ occurring when $a \sim 0.5l$. For $\alpha_z^x/c \simeq 0.3\chi$, $\alpha_y^x/c \simeq 0.3$ and $a \simeq 0.5l$, we get $\overline{\sigma_2} \simeq 10^{-6} l [\text{nm}] \text{ohm}^{-1} \text{volt}^{-1}$. In comparison, a nonlinear longitudinal conductivity of $10^{-3} \text{ohm}^{-1} \text{volt}^{-1}$ has been recently measured in chiral tellurium [28].

The preceding analysis can be extended to WSM with multiple pairs of valleys. For example, in a WSM with time-reversal symmetry, valleys related by \mathcal{T} have opposite tilts but the same chirality. Based on Eq. (23), those valleys make equal contributions to $\overline{j_{2,x}}$, thereby enhancing it.

Conclusion.— We have unveiled a mechanism for a nonlinear longitudinal current in non-magnetic wires of finite thickness, resulting from (i) non-specular scattering at wire surfaces; (ii) a Berry curvature of electrons in the direction orthogonal to both the transport and the wire surface; (iii) an energy dispersion that is asymmetric at each electronic valley along the directions orthogonal to transport. Conditions (i) and (ii) ensure a surface-localized current distribution, *quadratic* in the applied

electric field and parallel to the field. Condition (iii) enables a nonzero average of the nonlinear current density over the thickness of the wire. Skew-scattering and side-jump are not required.

We have illustrated our theory for Dirac and Weyl materials, where the effect can be sizeable. An experimental challenge is to distinguish the surface current predicted here from more conventional [22] but symmetry-allowed nonlinear bulk currents. Possible strategies include thickness- and electron-density-dependent conductance measurements or the use of local current probes [29] (see End Matter for an extended discussion).

Our study was limited to a wire that is spatially homogeneous in equilibrium. In real interconnects, the composition of the wire along its cross section is inhomogeneous. In such case, an inspection of Eq. (1) shows that the Berry curvature contributes to the longitudinal electric current at *first order* in the applied electric field. Although further work is needed to quantify this scenario, [there is a prospect to engineer smooth electron concentration gradients in interconnects in order to enhance their conductivity by virtue of the Berry curvature](#). Another future direction of research is to generalize our theory to the situation where the bulk states coexist with surface states, and intervalley scattering is not negligible.

Acknowledgements.— This work has been financially supported by the Canada First Research Excellence Fund, the Natural Sciences and Engineering Research Council of Canada (Grant No. RGPIN-2018-05385). We are grateful to C.-T. Chen, E. Lantagne-Hurtubise and A.-M. Tremblay for informative discussions.

-
- [1] D. Gall, *Journal of Applied Physics* **127**, 050901 (2020).
[2] D. Gall, J. Cha, Z. Chen, H. Han, C. Hinkle, J. Robinson, R. Sundararaman, and R. Torsi, *MRS Bulletin* **46**, 959 (2021).
[3] C. Zhang, Z. Ni, J. Zhang, X. Yuan, Y. Liu, Y. Zou, Z. Liao, Y. Du, A. Narayan, H. Zhang, *et al.*, *Nature materials* **18**, 482 (2019).
[4] M. Breitzkreuz and P. W. Brouwer, *Phys. Rev. Lett.* **123**, 066804 (2019).
[5] M. J. Gilbert, *Communications Physics* **4**, 70 (2021).
[6] N. A. Lanzillo, U. Bajpai, I. Garate, and C.-T. Chen, *Physical Review Applied* **18**, 034053 (2022).
[7] S.-W. Lien, I. Garate, U. Bajpai, C.-Y. Huang, C.-H. Hsu, Y.-H. Tu, N. A. Lanzillo, A. Bansil, T.-R. Chang, G. Liang, *et al.*, *npj Quantum Materials* **8**, 3 (2023).
[8] K. Fuchs, *Mathematical Proceedings of the Cambridge Philosophical Society* **34**, 100 (1938).
[9] E. H. Sondheimer, *Advances in Physics* **1**, 1 (1952).
[10] I. Sodemann and L. Fu, *Physical review letters* **115**, 216806 (2015).
[11] C. Ortix, *Advanced Quantum Technologies* **4**, 2100056 (2021).
[12] Q. Ma, S.-Y. Xu, H. Shen, D. MacNeill, V. Fatemi, T.-R. Chang, A. M. Mier Valdivia, S. Wu, Z. Du, C.-H. Hsu, *et al.*, *Nature* **565**, 337 (2019).
[13] K. Kang, T. Li, E. Sohn, J. Shan, and K. F. Mak, *Nature materials* **18**, 324 (2019).
[14] Q. Ma, A. G. Grushin, and K. S. Burch, *Nature materials* **20**, 1601 (2021).
[15] S. S. Tsirkin and I. Souza, *SciPost Phys. Core* **5**, 039 (2022).
[16] K. Das, S. Lahiri, R. B. Atencia, D. Culcer, and A. Agarwal, *Physical Review B* **108**, L201405 (2023).
[17] Y. Wang, Z. Zhang, Z.-G. Zhu, and G. Su, “An intrinsic nonlinear ohmic current,” (2023), [arXiv:2207.01182 \[cond-mat.mes-hall\]](#).
[18] D. Xiao, Y. Yao, Z. Fang, and Q. Niu, *Physical Review Letters* **97**, 026603 (2006).
[19] See Supplemental Material at [URL] for details of the analytical derivations and citations to Refs. [30–33].
[20] We have omitted any hypothetical internal electric field component in the z direction. In systems displaying a nonlinear Hall effect, an internal nonzero E_z would emerge, which would be quadratic in E_x . However, the source term produced by such a field in Eq. (10) would be even in p_x and hence irrelevant for transport along x .

- [21] This statement is in agreement with conventional theories (for a review, see e.g. Ref. [25]).
- [22] H. Isobe, S.-Y. Xu, and L. Fu, *Science advances* **6**, eaay2497 (2020).
- [23] D. Xiao, M.-C. Chang, and Q. Niu, *Reviews of modern physics* **82**, 1959 (2010).
- [24] R. Powell, *Symmetry, Group Theory, and the Physical Properties of Crystals*, Vol. 824 (2010).
- [25] Y. Gao, *Frontiers of Physics* **14**, 33404 (2019).
- [26] To leading order in α_z , $\bar{\sigma}_2/\bar{\sigma}_1 \simeq eh\alpha_z/(6\pi m^2)$ for $a \simeq l$.
- [27] N. Armitage, E. Mele, and A. Vishwanath, *Reviews of Modern Physics* **90**, 015001 (2018).
- [28] M. Suárez-Rodríguez, B. Martín-García, W. Skowroński, F. Calavalle, S. S. Tsirkin, I. Souza, F. De Juan, A. Chuvilin, A. Fert, M. Gobbi, F. Casanova, and L. E. Hueso, *Phys. Rev. Lett.* **132**, 046303 (2024).
- [29] K. C. Nowack, E. M. Spanton, M. Baenninger, M. König, J. R. Kirtley, B. Kalisky, C. Ames, P. Leubner, C. Brüne, H. Buhmann, *et al.*, *Nature materials* **12**, 787 (2013).
- [30] M. Dyakonov, *Physical Review Letters* **99**, 126601 (2007).
- [31] D. T. Son and N. Yamamoto, *Physical review letters* **109**, 181602 (2012).
- [32] A. M. Tremblay, B. Patton, P. C. Martin, and P. F. Maldague, *Phys. Rev. A* **19**, 1721 (1979).
- [33] A.-M. S. Tremblay and F. Vidal, *Phys. Rev. B* **25**, 7562 (1982).

END MATTER

Discussion: experimental detection

The main prediction of this work is a longitudinal, nonlinear, surface-localized current that is produced by the combined action of the bulk Berry curvature and diffusive boundary scattering. As we discuss next, there are challenges to unequivocally detect such current, but there may be viable paths ahead.

Overall, nonlinear currents can be experimentally distinguished from the dominant linear current, as done e.g. in Ref. [28]. Likewise, the spatial distribution of surface-localized currents can be mapped through SQUID measurements (see e.g. Ref. [29]).

A more fundamental challenge for the detection of our proposed current is that it coexists with *bulk* currents (i.e. currents that are distributed over the entire volume of the sample) predicted in Ref. [22]. The latter originate from the mechanism of skew-scattering, which appears in the collision term of the Boltzmann equation beyond our lowest Born approximation. At first thought, one could differentiate our surface-localized current from the bulk currents by measuring the scaling of the conductance with the wire thickness. If the wire is thick compared to the bulk mean free path, the contribution from the bulk currents of Ref. [22] to the measured conductance will scale linearly with the wire thickness. In contrast, our predicted contribution to conductance will be independent of the thickness.

There is a caveat, however. While the theory of Ref.

[22] was done for an infinite sample, it is likely that in finite wires it will be affected by diffusive boundary scattering. As a result, the contribution from skew-scattering to conductance may not be a perfectly linear function of the wire thickness. In this case, further analysis is required to distinguish the Berry curvature contribution to the current from the boundary-induced changes of the skew-scattering contribution to the current. To make matters more difficult, both currents have the same dependence on impurity concentration and on the scattering time. Fortunately, the dependence of the current on the carrier density is rather different depending on the mechanism at hand (Berry curvature vs skew-scattering). This is evident from comparing our expressions with those of Ref. [22]. Still, varying the electron density in a controllable way is not simple, especially in three dimensional materials.

An alternative approach consists of adopting a transport configuration in which bulk nonlinear longitudinal currents are forbidden by symmetry. Specifically, let us discuss the case of a transition metal dichalcogenide monolayer in the xy plane (the crystal orientations corresponding to x and y axes are illustrated in Ref. [22]; note that this nomenclature differs from the one we adopted in the main text, where the y direction was out-of-plane.)

In this system, a bulk nonlinear longitudinal current is allowed by symmetry when the electric field points along y , but not when it points along x . In the latter case, the energy dispersion at each valley is symmetric in the transverse direction ($\alpha_z^x = 0$ in Eq. (13)); this is the microscopic origin for the vanishing of the nonlinear longitudinal current along x .

Importantly, our calculations (Eqs. (11), (12) and Fig. 2a) show the existence of nonlinear currents produced by the Berry curvature at each electronic valley, even when the electric field points in the x -direction. These valley-resolved currents are spatially localized within a mean free path from the wire boundaries. But, at each boundary, the two valleys make mutually cancelling contributions to the nonlinear current along x .

Now, we may avoid such cancellation between valleys by breaking time-reversal symmetry at (and only at) the wire boundaries, e.g. with magnetic interfaces. In the theory of Fuchs and Sondheimer, this will result in a boundary condition that is no longer the same for the two valleys. Consequently, the cancellation between the valleys will be prevented and net currents produced by the Berry curvature will flow along x close the boundaries. In contrast, skew-scattering contribution to nonlinear current along x is expected to vanish separately at each valley, due to the very same symmetry that prevents bulk nonlinear currents ($\chi_{xxx}^{(1)} = 0$ in Ref. [22]). Moreover, the effect of boundary scattering being unimportant far from the boundary, the bulk currents will remain null therein. This way, one can experimentally confirm our predicted current by measuring a nonlinear conductance of the wire that is

independent of the wire thickness.

A final remark is in order here. Since the energy dispersion along the transport direction x is asymmetric in each valley, the time-reversal breaking boundary condition can generate an extra nonlinear current along x in the vicinity of the boundary, which is unrelated to both skew-scattering and to the Berry curvature (see e.g. Eq. (S46) in Ref. [22]). It is however feasible to distinguish such extra current from the one that emerges from the

Berry curvature. The key point that allows to do so is that the Berry curvature contribution to the current at a given valley changes sign between the top and bottom boundaries of the wire (see Fig. 2a), whereas the non-Berry contribution does not. Thus, by breaking time-reversal symmetry oppositely (with same magnitude but opposite sign) on the top and bottom boundaries, one can single out the geometric (Berry) contribution to the nonlinear longitudinal current.